New insulation aging detection algorithm for HV and MV cable based on the study of the harmonic content in leakage current

Javier **BENGOECHEA** de la Llera, Lumiker (RDT company), (Spain), javier.bengoechea@lumiker.com
Joachim **NIEMANN-LARSEN,** Energinet, (Denmark), jal@energinet.dk
Soumya **THAKUR**, Technical University of Denmark (DTU), (Denmark), south@dtu.dk,
Asier **GONZALEZ** ORTIZ, Lumiker (RDT company), (Spain), asier.gonzalez@lumiker.com

ABSTRACT

Early detection of degradation is crucial to prevent severe cable damage. This paper explores the possibility of using the cable screen currents as an indicator of cable aging status. A T-circuit model is developed for three single-core coaxial cables excited by three-phase voltages, where the XLPE insulation is modelled using a parallel conductance (G) and capacitance (C) branch representing a non-linear, voltage-dependent admittance. A set of differential equations are defined for the above configuration to describe the harmonic content of the leakage current under partial discharges as a result of insulation deterioration and water treeing.

KEYWORDS

Optical current transformer, harmonics, leakage current, partial discharge, water tree, XLPE cables, thermal aging, health index.

INTRODUCTION

With an increase in the need for a secure grid, the impact of unscheduled decommissioning of medium and high-voltage transmission cables is a subject of particular concern. This attracts high interest in researching aging studies of cables, in particular, that of its insulation. For this purpose, continuous monitoring of the cable condition is necessary. At present, two types of tests are available for detecting aging: tan delta measurements and partial discharge measurements [1] These tests have excellent detection accuracy but come with some challenges. The former requires taking the cable out of service and the latter involves the deployment of complex systems that require a power supply along the entire length of the cable. This indicates a need for developing a measurement technique that can detect aging while overcoming these drawbacks.

It is becoming increasingly common to have current measurement systems at cable screen earthing. The current content can be examined to explore the relationship between the cable age and the harmonic characteristics and content of the leakage current migrating through the cable insulation, which eventually is reflected in the frequency-resolved current content distribution in the cable screen. The deterioration of the XLPE insulation because of aging results in the generation of harmonics of specific (odd) orders in the leakage current, as a result of the non-linear behaviour of the XLPE insulation conductance. Water trees formed inside the XLPE insulation is one type of severe deterioration, and former studies have correlated non-linear dielectric responses as a result of water trees, with some focus being on the generation of third harmonics in the leakage (loss) current, where the harmonic current magnitude and phase angle has been shown to, respectively, increase and decrease with water tree degradation [2]–[4]. Furthermore, thermal aging has been shown to generate harmonics of especially third, sixth, and thirteenth order in the leakage current [5]. It is thus evident, that the non-linear V-I relationship of the XLPE insulation and associated harmonic current generation caused by water trees, is a promising diagnostic benchmark for the health of the cable insulation, where early detection is of great interest.

Due to the nature of the coaxial cable geometry, the generated harmonic content in the leakage current is reflected in both the phase conductor and screen conductor current flows, and thus any system-level harmonics that may be present in the cable conductor and screen voltages themselves or from inductive coupling from the other phases, must carefully be separated from the analysed harmonic current content generated by the insulation. The effects of said system-level harmonics are examined on the proposed circuit model of this paper.

The loss tangent, tan(δ), is commonly used to describe cable insulation health, and is basically the relationship between the resistive leakage current to the capacitive (charging) current, where for an ideal insulator, the former is zero, resulting in a phase difference of the two components equal to 90 degrees. As XLPE insulation ages, the loss tangent is seen to increase in value [6].

For water trees and insulation breakdown in general associated with partial discharge generation, the proposed circuit model in this paper adapts a parallel conductance/capacitance (GC) branch, where the conductance of idea cable insulation is zero, however, the generation of partial discharges can basically be seen as a degradation of this conductance (and to some degree capacitance), and the accumulation of these discharges can constitute a measurable (leakage) current. This current is, in principle, dependent on the operating voltage, since partial discharges only occur in certain areas of the voltage waveform. This current will therefore lead to an increase in the harmonic content of the screen current.

MODEL DESCRIPTION

The basis for the theoretical modelling is a simple circuit of 100 m of three single-core, high-voltage coaxial cables of 420 kV, 2500 mm^2 Al, excited by three-phase voltage sources at both ends. Any variation of phase at one end, results in a corresponding current flow, which can be as high as 100A as seen in a case study in this paper. The cable circuit screens are shorted, representing a double-point grounded screen configuration.

The development of circuit equations assumes that capacitances are restricted to a per-phase basis. Mutual inductive coupling is included for each phase to each screen, and between the three screens themselves, where that latter is considered due to the circulation of currents in the screens as a result of the double-ended grounding.

Single-phase circuit model

For simplicity, the governing equations are firstly developed for a single, isolated phase configuration with voltage excitation from one end, where the equivalent circuit can be seen in Figure 1 below. This circuit and its dynamic set of equations will be used as the basis of the computation of the conductance generated harmonics. The insulation "admittance" consists of capacitance (C) and conductance (G) forming the shunt connection in this T-model, with equal phase resistance (R) and self-inductance (L), and screen self-inductance (L_s) and resistance (R_s), plus mutual phase-to-screen inductive impedance couplings (M) on both side of the T branch. Grounding resistances, R_{gr}, of 1 ohm are introduced in the screen circuit, and are thus the limiting elements of the only path of screen current circulation. A high current induction transformer produces the current Ig in the looped conductor, while a voltage source V_g excites the potential between conductor and metallic screen. For the modelling/simulations, Vg will be excited with a proper harmonic content, representing system level harmonics.

Governing equations

This section describes the governing equations of the equivalent circuit (Figure 1). The intention is to mathematically solve the current flow through the shunt admittance of the insulation and relate the current magnitude and phase in the C component with the G component. This would allow for an analytical description of the distorted, harmonic current of the latter.

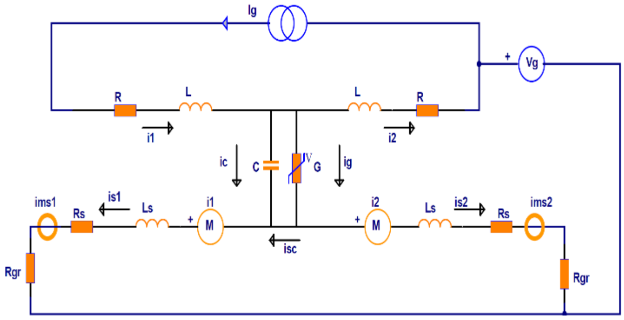

Figure 1: Equivalent circuit diagram of 1 single coaxial high voltage cable excited at one end.

The non-linear, voltage-dependent conductance, G, can have various approximations, however, the V-I characteristic is expected to be of cubic behaviour, with either a value equal to zero at zero voltage level, or a value equal to g_0 at zero voltage level. The value of the conductance must be positive as the passive component it is representing. Expressing the conductance (G) response, it can be defined as a polynomial whose variable is the terminal voltage (drop) of the conductance value, where the response should be symmetrical with reference to the voltage. Thus, the polynomial should only contain even powers. I.e., using the voltage across it, v_g, it should thus be on the form as given in Eq. (1) below:

$$G = g_0 + g_2 {v_g}^2 \qquad (1)$$

where g_0 is the conductance expressed as the reciprocal of the element, i.e., $g_0 = \frac{1}{R}$, similarly is g_2 where a constant *k* is introduced, i.e., $g_2 = \frac{k}{R}$. The current through the conductance, i_g, can then be computed from as shown in Eq. (2) below.

$$Gv_g = (g_0 + g_2 {v_g}^2) v_g \qquad (2)$$

which results in a cubic, non-linear V-I relationship that also is in accordance with a proposed approximation from lab specimens of bridged water trees provided in [7] of the form $\frac{1}{R}(v_g + k v_g^3)$. Note the odd (cubic) power of the V-I relationship in (2) above, indicating that the conductance only will generate harmonics of odd powers.

By inspecting the equivalent circuit of Figure 1, one can derive the following equation of the voltage drop across the L and R of the main conductor, which must be the same for each half, thus:

$$v_c = \; R i_2 + L \frac{di_2}{dt} + v_g \qquad (3)$$

Similarly, the total voltage drop across the M, Ls, and Rs of the screen, with each half being equal, can be expressed in two equations:

$$v_s = \; R_s i_{s2} + L_s \frac{di_{s2}}{dt} + M \frac{di_2}{dt}$$

$$v_s = \; R_s i_{s1} + L_s \frac{di_{s1}}{dt} - M \frac{di_1}{dt} \qquad (4)$$

Then, the voltage drop across the C and the voltage drop across the G must be equal as they are in parallel, which can be utilized to express a combined voltage drop, here denoted v_m where the subscript m denoted the "midpoint" of the T-branch, from the current through the C and the current though the G:

$$v_m = \frac{1}{C} \int i_c dt \qquad C \frac{dv_m}{dt} = i_c$$

$$v_m = \frac{i_g}{G_m} \qquad G_m v_m = i_g \qquad G_m = g_2 v_m^2 \qquad (5)$$

where the conductance expression, Gm, is from the definition earlier, but with the g_0 term for zero-value neglected.

By KCL on the formed current loops, and recognizing the connection through the (shorted) voltage source Vg, the following must be true:

$$i_1 - i_2 = i_c + i_g = i_{s1} + i_{s2} \qquad (6)$$

From the above set of equations, one may end up with the following differential equation:

$$v_g + Ri_g + L\frac{di_g}{dt} = v_m + R_tC\frac{dv_m}{dt} + L_tC\frac{d^2v_m}{dt^2} + g_2R_tv_m^3 + 3g_2L_tv_m^2\frac{dv_m}{dt}$$

(7)

where:

$$R_t = R + \frac{R_s}{2}$$
$$L_t = L + \frac{L_s}{2} - \frac{M}{2}$$

(8)

The first parts of Eq. (7) can be said to be the response in the case of a constant valued admittance, while the additional non-linear terms describe the non-linear response of the voltage-dependent conductance (or combined mid-point voltage of "admittance"). The equivalent admittance would be very small, likewise the g_2 constant. An explicit approaximation could be achieved, but numerical implicit integration is preferred as it is more flexible in case of the form of the admittance needs to be changed, where the Runge-Kutta 4th order method is a suitable choice.

Equations for the total voltage drops from the total circulation current in the screen circuit can also be developed for the computation of said total circulating screen current, I_{sc}, where firstly, by recognizing similar KCL relationship as before

$$i_c + i_g = i_{s1} + i_{s2} = 2i_s$$

(9)

the voltages of the closed-loop screen/ground mesh can be prescribed as below, where some of the main phase currents of each half, i_{s1} and i_{s2}, are coupled:

$$R_si_{s1} + L_s\frac{di_{s1}}{dt} - R_si_{s2} - L_s\frac{di_{s2}}{dt} + 2(R_s + R_{gr})i_{sc} + 2L_s\frac{di_{sc}}{dt} = M\frac{di_1}{dt} + M\frac{di_2}{dt}$$

(10)

Then, by assuming that $i_{s1} \cong i_{s2}$ and $i_1 \cong i_2$, Eq. (10) above can be simplified to:

$$2(R_s + R_{gr})i_{sc} + 2L_s\frac{di_{sc}}{dt} = 2M\frac{di_1}{dt}$$

(11)

By remembering $i_1 = I_g$, the solution to the rather simple differential equation of Eq. (11) above can readily be computed to:

$$I_{sc} = j\frac{\frac{M}{L_s}\omega}{\frac{R_{gr} + R_s}{L_s} + j\omega}I_g$$

(12)

By introduction of the grounding resistances, R_{gr}, the circulating current in the screen is limited, and from variation of the resistance value, a stable solution can be found, which for this case was the applicable for realistic values of 0.1-1 Ω. From Eq. (12) it is evident that at DC excitation (zero frequency), the total screen current, I_{sc}, would equal zero.

Note, that the differential equation (10) contains no non-linear terms of the conductance, and hence does not require the use of an indirect, time-dependent solving approach, as opposed to the previous terms containing the mid-point voltage v_m; instead Eq. (10) can be solved in steady-state as evident from Eq. (12).

Three-phase circuit model

While the previously analysed single-phase circuit above is used for the simulation of the harmonic current generation of the non-linear conductance, similar equations are here developed for a three-phase cable circuit. The proposed complete circuit model can be seen in Figure 2, where insulation admittance consisting of capacitance (C) and conductance (G_x) per phase is forming the shunt connection in the T model, with equal phase resistance (R) and self-inductance (L), and screen self-inductance (L_s) and resistance (R_s), plus mutual phase-to-screen and mutual screen-to-screen inductive impedance couplings on both side of the T branch. With phase a as an example, the mutual inductive impedance between phase a and screen a is represented as the Maa expression, the mutual inductive impedance between screen a, and phase b and c as the Mab and Mac expressions, respectively, while the couplings between screen a and the screens of b and c are

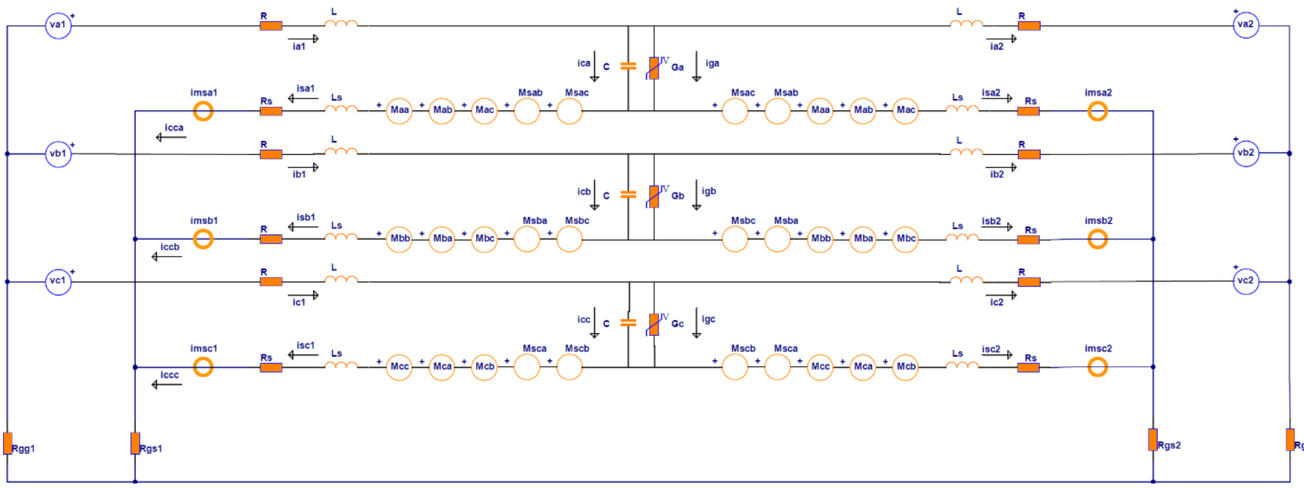

Figure 2: Equivalent circuit diagram of a 3 single core coaxial three-phase high voltage cables excited at both ends

represented by the expressions $Msab$ and $Msac$, respectively. Similarly for the remaining phases and screens. Grounding resistances of 0.1-1 Ω are introduced on each side of the screens.

Using the same terminology from the single-phase circuit and the same non-linear conductance of Eq. (1), equations are here developed for phase a of Figure 2, where the complexity of the equations and number of equations increase due to the three separate phases and screens, plus the different voltage excitations of each end.

Firstly, the two voltage sources (that can vary in magnitude and phase) can be expressed from summation of their enclosed voltage loops:

$$v_{a1} = \quad Ri_{a1} + L\frac{di_{a1}}{dt} + v_{am} + v_{sa1} + v_{rgs1} + v_{gg1}$$

$$v_{a2} = -Ri_{a2} - L\frac{di_{a2}}{dt} + v_{am} + v_{sa2} + v_{rgs2} + v_{gg2}$$

(13)

where the voltage drop, v_{am}, across the midpoint “admittance” and currents through the capacitance and conductance, i_{ca}, and i_{ga}, respectively, will be identical to the set of equations from Eq. (5), but this time with included g_0 constant.

And similarly, from KCL:

$$i_{a1} - i_{a2} = i_{ca} + i_{ga} = i_{sa1} + i_{sa2}$$

(14)

The voltage drops of each side of the screen, v_{sa1}, and v_{sa2} from Eq. (13) above, can by defining terms for the coupling currents between the screens of each phase, i_{cca}, i_{ccb}, and i_{ccc}, and with the coupling of some of the currents of the main phase currents, i_{a1}, i_{b1}, and i_{c1} (and similar for half 2), be expressed as:

$$\begin{aligned} v_{sa1} = R_s i_{sa1} + L_s\frac{di_{sa1}}{dt} + R_s i_{cca} + L_s\frac{di_{cca}}{dt} - M_{aa}\frac{di_{a1}}{dt} \\ - M_{ab}\frac{di_{b1}}{dt} - M_{ac}\frac{di_{c1}}{dt} + M_{sab}\frac{di_{sb1}}{dt} \\ + M_{sab}\frac{di_{ccb}}{dt} + M_{sac}\frac{di_{sc1}}{dt} + M_{sac}\frac{di_{ccc}}{dt} \end{aligned}$$

$$\begin{aligned} v_{sa2} = R_s i_{sa2} + L_s\frac{di_{sa2}}{dt} - R_s i_{cca} - L_s\frac{di_{cca}}{dt} + M_{aa}\frac{di_{a2}}{dt} \\ + M_{ab}\frac{di_{b2}}{dt} + M_{ac}\frac{di_{c2}}{dt} + M_{sab}\frac{di_{sb2}}{dt} \\ - M_{sab}\frac{di_{ccb}}{dt} + M_{sac}\frac{di_{sc2}}{dt} - M_{sac}\frac{di_{ccc}}{dt} \end{aligned}$$

(15)

Finally, the voltage drops of the screen grounding resistors and generator neutral star point resistors, v_{rgs1} and v_{gg1}, respectively, (and similar for half 2) from Eq. (13), can be defined as Eq. (17).

$$v_{rgs1} = R_{gs1}(i_{sa1} + i_{sb1} + i_{sc1} + i_{cca} + i_{ccb} + i_{ccc})$$

$$v_{rgs2} = R_{gs2}(i_{sa2} + i_{sb2} + i_{sc2} - i_{cca} - i_{ccb} - i_{ccc})$$

$$v_{gg1} = R_{gg1}(i_{sa1} + i_{sb1} + i_{sc1} + i_{a1} + i_{b1} + i_{c1})$$

$$v_{gg2} = R_{gg2}(i_{sa1} + i_{sb1} + i_{sc1} - i_{a2} - i_{b2} - i_{c2})$$

(17)

To calculate the mid-point voltage drop and currents (of the conductance and capacitance), the development of an equation for the sum of the two voltage sources is necessary. Therefore, by summation of the two expressions of Eq. (13) and rewriting:

$$\begin{aligned} v_{a1} + v_{a2} = \quad & RSi_{sa} + LDi_{sa} + 2v_{am} + R_s Si_{sa} + L_s Di_{sa} \\ & - M_{aa}Di_{sa} - M_{ab}Di_{sb} - M_{ac}Di_{sc} \\ & + M_{sab}Di_{sb} + M_{sab}Di_{sb} + 2(R_{gs} \\ & + R_{gg})Si_{sa} + 2(R_{gs} + R_{gg})Si_{sb} + 2(R_{gs} \\ & + R_{gg})Si_{sc} \end{aligned}$$

(18)

where:

$$Si_{sa} = i_{sa1} + i_{sa2} = \; C\frac{dv_{am}}{dt} + (g_0 + g_2 v_{am}^2)v_{am}$$

(19)

and its first derivative:

$$Di_{sa} = \frac{di_{sa1}}{dt} + \frac{di_{sa2}}{dt} = \; C\frac{d^2 v_{am}}{dt^2} + (3g_2 v_{am})v_{am}$$

(20)

Eq. (18) can similarly be defined for phase b and c, and the complete set of equations be put in matrix form, which has been done in Eq. (16) shown at the bottom of this page.

The variables to be determined are thus the mid-point voltages of all three phases, denoted x: v_{xm}, which only depend on the values of v_{x1} and v_{x2}.

The solution of this system first involves the diagonalising of the matrix with the second derivatives, after which the Runge-Kutta method of 4th order again can be utilised.

Like that of the single-phase circuit, expressions for the circulating currents of the three-phase circuit, i_{cca}, i_{ccb}, and i_{ccc} must be setup. By KVL, the voltage dropped in the combined screen-to-neutral circuit can be expressed as:

$$\begin{aligned} M_{aa}\frac{di_{a1}}{dt} + M_{ab}\frac{di_{b1}}{dt} + M_{ac}\frac{di_{c1}}{dt} - M_{sab}\frac{di_{sb1}}{dt} - M_{sab}\frac{di_{sc1}}{dt} \\ + +M_{aa}\frac{di_{a2}}{dt} + M_{ab}\frac{di_{b2}}{dt} + M_{ac}\frac{di_{c2}}{dt} \\ + M_{sab}\frac{di_{sb2}}{dt} + M_{sab}\frac{di_{isc2}}{dt} \\ = \; 2R_s i_{cca} + 2L_s\frac{di_{cca}}{dt} + (R_{gs1} \\ + R_{gs2})(i_{cca} + i_{ccb} + i_{ccc}) \end{aligned}$$

$$\begin{bmatrix} v_{a1}+v_{a2} \\ v_{b1}+v_{b2} \\ v_{c1}+v_{c2} \end{bmatrix} = \begin{bmatrix} 2+(R+R_s+R_{gs}+2R_{gg})g_0 & (R_{gs}+2R_{gg})g_0 & (R_{gs}+2R_{gg})g_0 \\ (R_{gs}+2R_{gg})g_0 & 2+(R+R_s+R_{gs}+2R_{gg})g_0 & (R_{gs}+2R_{gg})g_0 \\ (R_{gs}+2R_{gg})g_0 & (R_{gs}+2R_{gg})g_0 & 2+(R+R_s+R_{gs}+2R_{gg})g_0 \end{bmatrix} \begin{bmatrix} v_{am} \\ v_{bm} \\ v_{cm} \end{bmatrix} + C\begin{bmatrix} R+R_s+R_{gs}+2R_{gg} & R_{gs}+2R_{gg} & R_{gs}+2R_{gg} \\ R_{gs}+2R_{gg} & R+R_s+R_{gs}+2R_{gg} & R_{gs}+2R_{gg} \\ R_{gs}+2R_{gg} & R_{gs}+2R_{gg} & R+R_s+R_{gs}+2R_{gg} \end{bmatrix} \begin{bmatrix} \frac{dv_{am}}{dt} \\ \frac{dv_{bm}}{dt} \\ \frac{dv_{cm}}{dt} \end{bmatrix} + C\begin{bmatrix} L+L_s-M_{aa} & M_{sab}-M_{ab} & M_{sac}-M_{ac} \\ M_{sba}-M_{ba} & L+L_s-M_{bb} & M_{sbc}-M_{bc} \\ M_{sca}-M_{ca} & M_{scb}-M_{cb} & L+L_s-M_{cc} \end{bmatrix} \begin{bmatrix} \frac{d^2v_{am}}{dt^2} \\ \frac{d^2v_{bm}}{dt^2} \\ \frac{d^2v_{cm}}{dt^2} \end{bmatrix}$$

$$+ g_2\begin{bmatrix} (R+R_s+R_{gs}+2R_{gg})v_{am}^2 & (R_{gs}+2R_{gg})v_{bm}^2 & (R_{gs}+2R_{gg})v_{cm}^2 \\ (R_{gs}+2R_{gg})v_{am}^2 & (R+R_s+R_{gs}+2R_{gg})v_{bm}^2 & (R_{gs}+2R_{gg})v_{cm}^2 \\ (R_{gs}+2R_{gg})v_{am}^2 & (R_{gs}+2R_{gg})v_{bm}^2 & (R+R_s+R_{gs}+2R_{gg})v_{cm}^2 \end{bmatrix} \begin{bmatrix} v_{am} \\ v_{bm} \\ v_{cm} \end{bmatrix} + 3g_2\begin{bmatrix} (L+L_s-M_{aa})v_{am}^2 & (M_{sab}-M_{ab})v_{bm}^2 & (M_{sac}-M_{ac})v_{cm}^2 \\ (M_{sba}-M_{ba})v_{am}^2 & (L+L_s-M_{bb})v_{bm}^2 & (M_{sbc}-M_{bc})v_{cm}^2 \\ (M_{sca}-M_{ca})v_{am}^2 & (M_{scb}-M_{cb})v_{bm}^2 & (L+L_s-M_{cc})v_{cm}^2 \end{bmatrix} \begin{bmatrix} \frac{dv_{am}}{dt} \\ \frac{dv_{bm}}{dt} \\ \frac{dv_{cm}}{dt} \end{bmatrix}$$

(16)

(21)

Eq. (21) can be simplified by assuming that $i_{sb1} \approx i_{sb2}$ and $i_{sc1} \approx i_{sc2}$, i.e.:

$$M_{aa}\left(\frac{di_{a1}}{dt}+\frac{di_{a2}}{dt}\right)+M_{ab}\left(\frac{di_{b1}}{dt}+\frac{di_{b2}}{dt}\right)+M_{ac}\left(\frac{di_{c1}}{dt}+\frac{di_{c2}}{dt}\right) = (2R_s+R_{gs1}+R_{gs2})i_{cca}+2L_s\frac{di_{cca}}{dt} + (R_{gs1}+R_{gs2})(i_{ccb}+i_{ccc})$$

(22)

Defining the below equations:

$$i_a = i_{a1}+i_{a2}$$
$$i_b = i_{b1}+i_{b2}$$
$$i_c = i_{c1}+i_{c2}$$

(23)

then Eq. (22) can be written in a more compact matrix form:

$$\begin{bmatrix} M_{aa} & M_{ab} & M_{ac} \\ M_{ba} & M_{bb} & M_{bc} \\ M_{ca} & M_{cb} & M_{cc} \end{bmatrix}\begin{bmatrix} \frac{di_a}{dt} \\ \frac{di_b}{dt} \\ \frac{di_c}{dt} \end{bmatrix} = 2\begin{bmatrix} R_s+R_{gs} & R_{gs} & R_{gs} \\ R_{gs} & R_s+R_{gs} & R_{gs} \\ R_{gs} & R_{gs} & R_s+R_{gs} \end{bmatrix}\begin{bmatrix} i_{cca} \\ i_{ccb} \\ i_{ccc} \end{bmatrix} + 2L_s\begin{bmatrix} 1 & 0 & 0 \\ 0 & 1 & 0 \\ 0 & 0 & 1 \end{bmatrix}\begin{bmatrix} \frac{di_{cca}}{dt} \\ \frac{di_{ccb}}{dt} \\ \frac{di_{ccc}}{dt} \end{bmatrix}$$

(24)

From Eq. (24) it is evident that the three phase currents, denoted subscript x, i_x, by default are well balanced from the equal resistances of the screens and ground circuits and the self-impedances. If the mutual impedances are equal also, the circulating screen currents will be balanced also, which could be the case for cables in trefoil formation.

To solve the above equations, it is necessary to define the following for the phase circuits:

$$[v_{a1}-R_{gs1}(i_{a1}+i_{b1}+i_{c1})]-[v_{a2}-R_{gs2}(i_{a2}+i_{b2}+i_{c2})] = Ri_{a1}+L\frac{di_{a1}}{dt}+Ri_{a2}+L\frac{di_{a2}}{dt}$$

(25)

Similar to the single-phase calculation of the circulating current, no non-linear element is here present, and the solution to the above differential equation can be performed as a steady-state problem, that eventually takes the solution as given in Eq. (26) below:

$$\begin{bmatrix} i_{cca} \\ i_{ccb} \\ i_{ccc} \end{bmatrix} = j\frac{\omega}{2}Z_{sg}^{-1}\begin{bmatrix} M_{aa} & M_{ab} & M_{ac} \\ M_{ba} & M_{bb} & M_{bc} \\ M_{ca} & M_{cb} & M_{cc} \end{bmatrix}Z_{xg}^{-1}\begin{bmatrix} v_{a1}-v_{a2} \\ v_{b1}-v_{b2} \\ v_{c1}-v_{c2} \end{bmatrix}$$

(26)

where:

$$Z_{sg} = \begin{bmatrix} R_s+R_{gs}+j\omega L_s & R_{gs} & R_{gs} \\ R_{gs} & R_s+R_{gs}+j\omega L_s & R_{gs} \\ R_{gs} & R_{gs} & R_s+R_{gs}+j\omega L_s \end{bmatrix}$$

$$Z_{xg} = \begin{bmatrix} R+R_{gg}+j\omega L & R_{gg} & R_{gg} \\ R_{gg} & R+R_{gg}+j\omega L & R_{gg} \\ R_{gg} & R_{gg} & R+R_{gg}+j\omega L \end{bmatrix}$$

Again, as seen, a frequency of 0 Hz will result in no inductive circulating current, adhering to the circuit theory.

RESULTS

The Runge-Kutta method of 4th order with properly defined auxiliary variables has been programmed in MATLAB to solve for v_m, i_g, i_c from the set of equations developed for the single-phase circuit, more specifically the differential equation of Eq. (7), while taking into consideration the expression of the circulation current of Eq. (12) as well.

In Figure 3 the computed current in the conductance, i_g, the capacitive current, i_c, the inductive coupling current, I_{sc}, and the total screen circulating current, $I_{sc} + I_{s1}$ is plotted. The initial behavior of the curves is the stabilization of the integration of the (transient) solution.

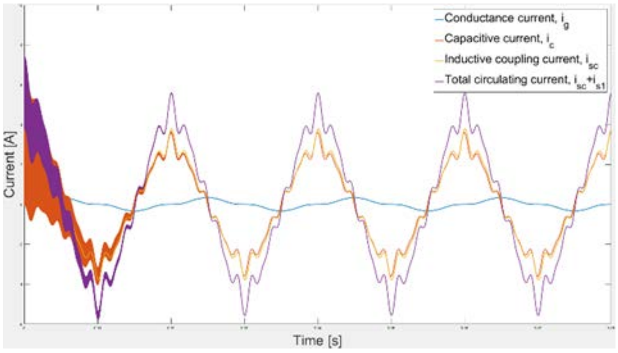

Figure 3: Computation of the conduction current, capacitive current, inductive coupling current, and the total screen circulating current.

From Figure 3 i_g (blue) can be seen to contain harmonics, especially the 3rd harmonic waveform. The conductance current is as expected 90° out of phase with the capacitive (and thus in phase with the generator voltage). As previously described, the generator voltage is defined to contain harmonics up until the 13th order, which are reflected in the capacitive current as well, as well as the circulating screen current. The generator harmonics contribute very little to the conductance current, which instead is dominated by its own generation of harmonics (especially of 3rd order).

To get a more clear distinction between generator harmonics and conductance generated harmonics, a FFT is performed and the percentage THD of the harmonic orders are plotted in Figure 4 below, where both the mid-point voltage harmonics and the conductance current harmonics are plotted, where the first is referenced to the total mid-point voltage and the latter to the total conductance current.

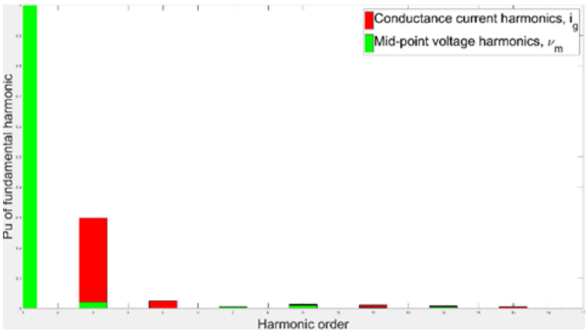

Figure 4: Percentage THD of mid-point voltage (green) and conductance current (red), each with ref. to its own fundamental.

Figure 4 proves that the harmonic current generation of the non-linear conductance is dominating the generation of odd current harmonics.

DISCUSSION

The proposed differential equations for the computation of the harmonic currents generated by the equivalent shunt conductance should be verified by experimental testing that includes thermal aging and water trees of/in the XLPE insulation, which is planned as the next steps by the authors of the paper. The no-linear V-I relationship in case of water tree has already been proven in previous work [4], [7], but it should be further researched to classify the amount of sensitivity of the harmonic current generation. A more detailed representation can be made to include hysteresis of the leakage current generation.

From optimised placement of current transformers (CTs) with sufficient bandwidth, e.g., passive, optical CTs around grounding link cables of a HV cable system, the harmonic current content of the screen currents to earth can be analysed, and combined with phase optical CT measurements, the harmonics of the leakage current can be separated from system harmonics in the main conductors, which as shown, also is mixed into the leakage and capacitive (charging) currents. The leakage current harmonic content can then from analysed lab results be used to give an early indication of insulation deterioration in an on-line measurement scheme. From thermal aging of XLPE insulation results in very high THD of especially the 3rd, 9th, and 13th harmonics of the leakage current, which emphasises the usability of a measurement scheme for early insulation deterioration detection [5]. One can even imagine that a sudden increase in harmonic leakage current content can indicate a pre-fault state.

The given equations can be expanded to single-point bonded cable systems, where the equivalent ground resistance values of the already provided double-point bonded system can be increased sufficiently. Finally, equations for a cross-bonded cable system can be developed, where circulating currents may or may not arise in the screens. For a cross-bonded scheme, an ingenious measurement scheme should be researched, such that leakage current measurements are properly captured, which can be difficult for a cross-bonded system with coaxial link cables.

CONCLUSION

The circuit model and developed differential equations presented in this paper shows that the nonlinear V-I characteristics of degraded XLPE insulation introduces harmonic currents in the leakage current. Thus, the measurement of leakage current in the earthing connection of power cable screens and the analysis of harmonics of specific order would enable an ageing detection method, which could be executed without taking the cable out of service.

In the future, the developed model is expected to be experimentally verified through a laboratory test of a power cable exposed to thermal degradation. The conductor and screen current shall be measured an analysed in different degradation stages to compare the harmonic content of the leakage current with the simulation, for the optimal development of an on-line algorithm for XLPE deterioration detection.

REFERENCES

[1] L. Li and J. Yong, "A new method for on-line cable tanδ monitoring," in *2018 18th International Conference on Harmonics and Quality of Power (ICHQP)*, IEEE, May 2018, pp. 1–6. doi: 10.1109/ICHQP.2018.8378870.

[2] N. Hussain, N. M. Nor, M. F. Abdullah, K. Ashraf, and A. Mirza, "Simulation of water tree distribution in medium voltage power cable insulation model in MATLAB/simulink," in *2014 5th International Conference on Intelligent and Advanced Systems (ICIAS)*, IEEE, Jun. 2014, pp. 1–5. doi: 10.1109/ICIAS.2014.6869554.

[3] Y. Yagi, H. Tanaka, and H. Kimura, "Study on diagnostic method for water treed XLPE cable by loss current measurement," in *1998 Annual Report Conference on Electrical Insulation and Dielectric Phenomena (Cat. No.98CH36257)*, IEEE, 1998, pp. 653–656. doi: 10.1109/CEIDP.1998.732982.

[4] F. N. Lima, J. C. Oliveira, D. A. Andrade, R. M. T. Silva, A. P. Finazzi, and B. C. Carvalho, "Modeling water tree phenomenon for insulated cable loss current estimation," in *2008 IEEE/PES Transmission and Distribution Conference and Exposition: Latin America*, IEEE, Aug. 2008, pp. 1–6. doi: 10.1109/TDC-LA.2008.4641816.

[5] Y. Liu, H. Wang, H. Zhang, and B. Du, "Thermal Aging Evaluation of XLPE Power Cable by Using Multidimensional Characteristic Analysis of Leakage Current," *Polymers (Basel)*, vol. 14, no. 15, p. 3147, Aug. 2022, doi: 10.3390/polym14153147.

[6] T. Tsujimoto, M. Nakade, Y. Yagi, K. Adachi, and H. Tanaka, "Development of on-site diagnostic method for XLPE cable by harmonics in AC loss current," in *Proceedings of the 7th International Conference on Properties and Applications of Dielectric Materials (Cat. No.03CH37417)*, IEEE, pp. 73–76. doi: 10.1109/ICPADM.2003.1218356.

[7] Y. Yagi, H. Tanaka, and H. Kimura, "Study on diagnostic method for water treed XLPE cable by loss current measurement," in *1998 Annual Report Conference on Electrical Insulation and Dielectric Phenomena (Cat. No.98CH36257)*, IEEE, pp. 653–656. doi: 10.1109/CEIDP.1998.732982.